Open Access **Baghdad Science Journal** **P-ISSN: 2078-8665**
Published Online First: May, 2023 **2024, 21(1): 62-71** **E-ISSN: 2411-7986**

DOI: https://dx.doi.org/10.21123/bsj.2023.8087

Enhanced Photocatalytic Activity of Cu_2O/ZnO/GO Nanocomposites on the Methylene Blue Degradation

Frikson Jony Purba*[1]** ***Zuriah Sitorus*[1]** ***Kerista Tarigan*[1] ***Nurdin Siregar*[2]**

[1]Department of Physics, Faculty of Mathematics and Natural Sciences, Universitas Sumatera Utara, Padang Bulan, 20155, Medan, Indonesia.
[2]Department of Physics, Faculty of Mathematics and Natural Sciences, Universitas Negeri Medan, Kenangan Baru, 20221, Medan, Indonesia.
*Corresponding author: kerista@usu.ac.id
E-mail addresses: purbafrikson@gmail.com, zuriah@usu.ac.id, siregarnurdin@unimed.ac.id

Received 10/11/2022, Revised 28/4/2022, Accepted 30/4/2022, Published Online First 20/5/2023, Published 01/1/2024

Abstract:

This study synthesized nanocomposite photocatalyst materials from a mixture of Cu_2O nanoparticles, ZnO nanoparticles, and graphene oxide (GO) through coprecipitation and hydrothermal methods. This study aims to determine the optimum composition of Cu_2O/ZnO/GO nanocomposites in degrading methylene blue. The nanocomposite was synthesized in two steps: 1 the synthesis of Cu_2O and ZnO nanoparticles through the coprecipitation method and the preparation of GO through the modified Hummer method. 2 The preparation of Cu_2O and ZnO nanoparticles mixtures with GO through the hydrothermal method to form Cu_2O/ZnO/GO nanocomposites. The adsorption-photocatalysis process of methylene blue was done with UV light from a halogen lamp. The characterization results indicated that the optimum composition was Cu_2O/ZnO nanocomposite with a ratio of 1:2 and 10% of GO, which had a specific surface area of 35.874 $m^2 g^{-1}$, a pore radius of 19.073 nm, and a pore volume of 0.092 $cm^3 g^{-1}$, and a diameter crystalline of 31.19 nm. The degradation efficiency of methylene blue under UV light for 120 minutes were 82.0%, 86.0%, 91.4%, and 79.3% using the Cu_2O/ZnO nanocomposites with GO of 1%, 3%, 5%, and 10%, respectively. These results indicated that Cu_2O/ZnO/GO nanocomposites efficiently degrade methylene blue from textile dye waste.

Keywords: Graphene oxide, Methylene blue, Nanocomposite, Photocatalytic activity, Textile dye waste degradation.

Introduction:

The higher activity of the textile industry's development indirectly affects the degradation of environmental quality, especially the generating of polluted water during industrial processes[1]. Most textile industries rely heavily on organic dyes in their dyeing processes[2]. This is extremely harmful if dye waste is released directly into a river without being treated, as the waste will become environmentally toxic and difficult to degrade naturally[3, 4]. Another issue is the increasing demand for clean water, resulting in large amounts of wastewater. As a result, wastewater treatment has become one of the decade's biggest challenges[5].

Generally, textile industry waste contains many azo dyes, compounds with benzene rings[6]. These dyes can be classified as reactive, acid, direct, basic, mordant, disperse, pigment, vat, anionic and ingrain, sulfur, solvent, and disperse dye[7]. Several purification procedures, such as adsorption, coagulation, and advanced oxidation, have been used to reduce the effluent, which contains a variety of dyes in significant amounts, considering the dye's stability and potential toxicity in water[8]. Advanced oxidation is a promising technique because it can transform chemical structures in various contaminated wastewater via oxidation processes to become hydroxyl radicals[9].

Compared to other advanced oxidation processes such as ozonation, fenton, and adsorption, heterogeneous photocatalysis is more cost-effective to produce a rapid oxidative reaction, free of toxic compounds, and environmentally benign[10]. Waste treatment methods via photocatalytic degradation can effectively lower organic dye levels. Among the various types of photocatalysis, many researchers

have focused their attention on semiconductor materials such as titanium dioxide (TiO_2), zinc oxide (ZnO), and copper oxide (Cu_2O)[11]. Among these semiconductor materials, the photocatalytic degradation capability of Cu_2O is of significant interest, as Cu_2O is an environmentally friendly p-type semiconductor material with a band gap energy (Eg) of approximately 2.0-2.2 eV, implying that the degradation activity is relatively high[12]. In addition, Cu_2O photocatalysis can be carried out with the assistance of sunlight[13]. However, like other semiconductor materials, pure Cu_2O exhibits a poor photocatalytic degradation capacity for organic dyes, such as Methylene Blue (MB)[14]. The degradation of MB via photocatalysis is based on the fast recombination of electron-hole pairs upon light absorption[15]. Thus, photocatalytic degradation by Cu_2O primarily aims to separate the electrons and holes generated by light absorption.

An alternative method for increasing the efficiency of photocatalytic degradation by Cu_2O is by incorporating additional materials as electron acceptors[16]. Numerous materials, including n-type semiconductors (ZnO and TiO_2), the conductive polymer polyaniline (PANI), graphene, and graphene oxide (GO), have been utilized to synthesize photocatalysts based on Cu_2O composites[17, 18]. Regarding this, ZnO is very promising as a supporting material for Cu_2O composites because ZnO has a band gap of 3.2 eV, a binding energy of 60 MeV, and an efficient electron-hole separation[19]. Besides, GO is a semiconductor material (sp^2 hybridization structure) that exhibits chromophoric properties, allowing it to absorb free electrons rapidly[20]. Therefore, the electron generated by Cu_2O can easily be transported to GO, avoiding the recombination of electron and hole pairs[21].

Furthermore, since the GO surface comprises chemical bonds with oxygen, it is well suited for the adsorption of organic dyes, enhancing the composite's photocatalytic degradation efficiency. Different investigations have used a combination of Cu_2O photocatalysts, ZnO, and GO for the degradation of dye materials, as demonstrated in Zou et al.[22], Ma et al.[23], and Huang et al.[24]. Thus, based on the advantages of each material, ZnO and GO seem to be very promising as supporting materials for enhancing the photocatalytic degradation efficiency of Cu_2O-based nanocomposites against methylene blue. This work is significant in providing an environmentally-friendly and rapid method as an alternative to reduce dye effluents, such as methylene blue. This research further furnishes the most recent discoveries of the potency of employing this nanocomposite with a considerable decomposition rate. This study aims to determine the most effective composition of Cu_2O/ZnO/GO nanocomposites for the degradation of methylene blue as an elaboration for our previous work[25].

Materials and Methods:

Materials

The materials used in this study were natural graphite, polyvinylpyrrolidone (PVP) (Merck), ethylene glycol (EG; Merck), copper(II) nitrate ($Cu(NO_3)_2.3H_2O$; Merck), silver nitrate ($AgNO_3$; Merck), zinc nitrate ($Zn(NO_3)_2.6H_2O$; Merck), trisodium citrate dihydrate ($C_6H_5Na_3O_7.2H_2O$; Merck), sulfuric acid (H_2SO_4 98 wt%; Merck), potassium permanganate ($KMnO_4$; Merck), sodium hydroxide (NaOH; Merck), hydrogen peroxide (H_2O_2 30 wt%; Merck) ethanol, and methylene blue (Merck).

Instrumentation

X-ray diffraction (XRD, Shimadzu Analytical Type 600) was used to determine physical properties, notably the crystal structure. Field-emission scanning electron microscope (FESEM) was employed to assess surface morphology and elemental content. Brunauer-Emmett-Teller analyzer (BET Sorption Analyzer NOVA 1000) was used to analyze specific surface area, pore volume, and pore size. In addition, fourier transform infrared spectroscopy (FTIR, Perkin Elmer Spectrum One) was used to determine functional groups of materials. Ultraviolet-visible spectroscopy (UV-Vis, Perkin Elmer) was used to determine the optical properties, including the absorbance value and energy gap. Meanwhile, photoluminescence spectroscopy was used to assess photocatalytic performance, specifically photocatalytic degradation activity.

Procedure

Preparation of Cu_2O Nanoparticles:

Cu_2O nanoparticles were synthesized through the coprecipitation method using $Cu(NO_3)_2.3H_2O$ precursor as a source for Cu^{2+} ions. The procedure followed Regmi et al.[26] with some modifications. Five grams of $Cu(NO_3)_2.3H_2O$ were dissolved in distilled water. Then, 0.2 g of PVP was dissolved in EG at 40 °C. The $Cu(NO_3)_2.3H_2O$ solution was then added to the PVP/EG solution and stirred for 30 minutes at 180 °C. After homogenization, the solution was centrifuged and rinsed three times using distilled water and ethanol. After that, the material was dried for 12 hours at 60 °C to obtain Cu_2O nanoparticle powder.

Preparation of ZnO Nanoparticles:

ZnO nanoparticles were synthesized by dissolving 3 mmol of $Zn(NO_3)_2.6H_2O$ in 50 mL of distilled water. Then, 6 mmol of $C_6H_5Na_3O_7.2H_2O$ (sodium citrate) was gently added to the solution while stirring until it turned transparent. Sodium citrate was added to increase the interlayer spacing of ZnO nanoparticles along the c-axis[27]. Then, up to 10 mL of 0.1 M NaOH was added dropwise under stirring for 60 minutes at room temperature. The precipitate was then centrifuged and neutralized with distilled water and ethanol to get pure ZnO nanoparticles. After washing, the precipitate was dried in an oven at 60 °C.

Preparation of GO:

The modified Hummer method was applied to prepare GO[28]. Two grams of graphite powder were dissolved in 98 mL of 98% H_2SO_4, and 4 g of $NaNO_3$ were added after 1 hour of stirring. After 2 hours of stirring, 8 grams of $KMnO_4$ was gradually added to the mixture. The stirring was stopped after 24 hours. The mixture was then washed using distilled water, and the remaining $KMnO_4$ was removed using H_2O_2. After that, the mixture was centrifuged and washed with HCl and distilled water to neutralize pH and remove any remaining SO^{2-} ions. The mixture was then dried at 110 °C for 12 hours to obtain graphite oxide sheets. 40 mg of graphite oxide was dissolved in distilled water and then ultrasonifying for 90 minutes at 50/60 Hz. Finally, graphite oxide was reduced by adding 0.8 g of Zn metal and 35% HCl and stirring for 1 hour to obtain GO.

Photocatalytic Testing:

To obtain the optimal composition of Cu_2O/ZnO/GO nanocomposites, the ratio of Cu_2O:ZnO nanoparticles was varied using the hydrothermal method in 1:1, 1:2, and 2:1. After determining the optimal ratio (based on our previous study[25], it was 1:2), the GO composition used in the nanocomposite was determined by varying into 1%, 3%, 5%, and 10%. Photocatalytic testing was conducted using UV light from a halogen lamp. The optimal wavelength of 664 nm was used for this procedure. The photocatalytic reaction was initiated by adding Cu_2O/ZnO/GO nanocomposites to 40 mL of 5 mg L^{-1} MB solution. The mixture was sonicated and then stirred in the darkness. The solution was exposed to UV light for 120 minutes while constantly stirred. Each solution was taken in 4 mL increments of 10, 30, 60, 90, and 120 minutes and then centrifuged. The absorbance of the supernatant was then measured to evaluate the reaction rate of the methylene blue degradation.

Results and Discussion:

XRD Characterization

XRD analysis examined the X-ray diffraction pattern formed by each Cu_2O/ZnO/GO nanocomposite sample after GO doping. As illustrated in Fig. 1, the difference in peaks from XRD data for Cu_2O/ZnO/GO nanocomposites (Cu_2O:ZnO = 1:2) with 1%, 3%, 5%, and 10% GO additions is almost non-significant.

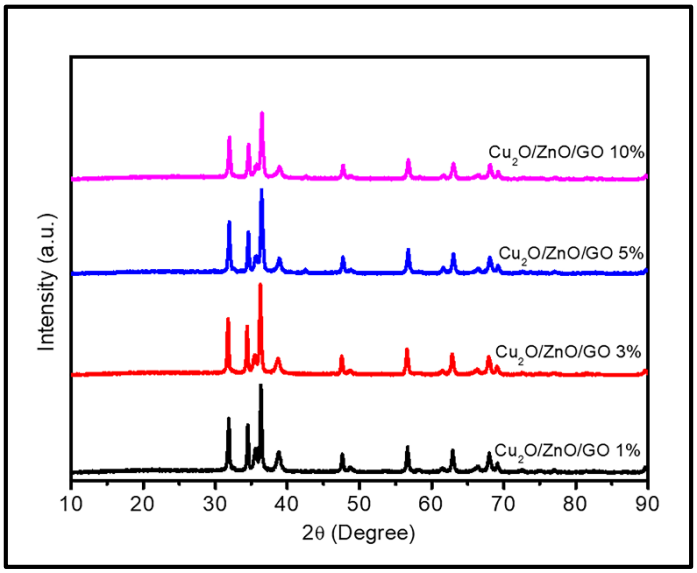

Figure 1. The X-ray diffraction pattern of Cu_2O/ZnO/GO nanocomposites.

The size of the distributed particles in the Cu_2O/ZnO/GO nanocomposites can be determined using the diffractogram by calculating the FWHM (full width at half maximum) from the pattern peak using the Scherrer equation approach (Equation 1)[29]. The crystallization size (D) of ZnO nanoparticles in Cu_2O/ZnO/GO nanocomposites at the highest diffraction pattern peak was calculated,

and the results are shown in Table 1. Furthermore, since other peaks excluded from Table 1 were considered as ZnO with low intensities, the corresponding data were not provided.

$$D = \frac{k\lambda}{\beta\cos\theta} \qquad 1$$

where D is the crystallite size (nm), k is the shape factor (0.9), β is full width at half maximum of peak (FWHM), λ is X-ray wavelength (0.154 nm), and θ is diffraction angle (radians).

Table 1. The diameter size of ZnO crystals distributed in Cu_2O/ZnO/GO nanocomposites.

Sample	2θ	FWHM	D (nm)
Cu_2O/ZnO/GO 1%	36.26°	0.36	24.26
Cu_2O/ZnO/GO 3%	36.23°	0.32	27.29
Cu_2O/ZnO/GO 5%	36.24°	0.28	31.19
Cu_2O/ZnO/GO 10%	36.23°	0.28	31.19

Note: Cu_2O:ZnO = 1:2

According to the findings, increasing the amount of GO in the nanocomposite causes a growth in the size of the ZnO crystals, which comes out to 24.26, 27.29, 31.19 and 31.19 nm for 1, 3, 5, and 10% of GO, respectively. Hence, it is reasonable to propose that the rGO sheets play a role in the growth of nanocrystals and act as nucleation centers and templates. This can cause the nanocrystals to grow on specific sites and directions, ultimately changing the material's morphology and close contact between CuO and ZnO nanoparticles[30]. This occurred because of the mutual attraction between Cu^+ and GO on ZnO. Despite this, the crystal size of the sample with 5% GO and that with 10% GO shows the same value. This could be because the amount of GO that can occupy Cu_2O/ZnO has reached its max amount, meaning that adding more GO will not significantly impact the crystal's size. In addition, the larger crystal size can potentially speed up the charge carrier process that results from the absorption of photon energy to carry out photocatalytic activity optimally[31], thereby increasing the ability to adsorb methylene blue compounds.

FESEM Morphology

FESEM analysis was performed on Cu_2O/ZnO/GO nanocomposites with GO additions of 1%, 3%, 5%, and 10%. This analysis aimed to evaluate the surface morphology of nanocomposites, as presented in Fig. 2. The results of the FESEM examination yielded an image of reduced graphene oxide nanosheets with a layered structure[25].

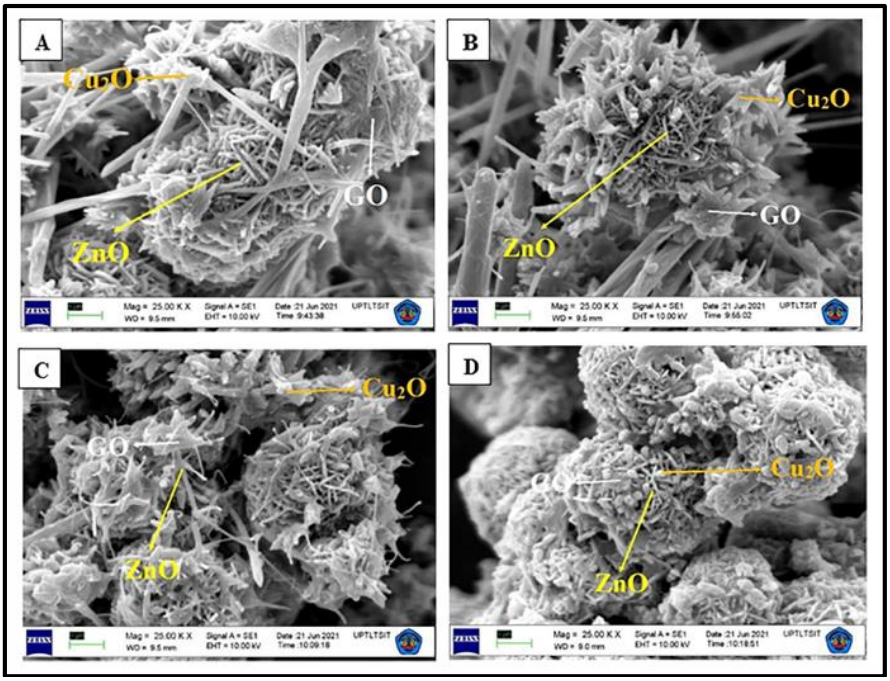

Figure 2. Morphology of Cu_2O/ZnO/GO nanocomposites (Cu_2O:ZnO = 1:2) with the addition of GO at a composition of (a) 1%, (b) 3%, (c) 5%, and (d) 10% at 25,000× magnification.

According to morphology analysis, GO appears to be composed of thinner sheets that are accumulating due to the chemical exfoliation of graphite oxide. The surface of the Cu_2O/ZnO nanoparticles is well decorated with GO nanosheets, as demonstrated by the SEM images prominently and clearly. In the meantime, Cu_2O nanoparticles are still present in nanocubes attached to the surface of ZnO and scattered throughout the surface. In addition to this, ZnO nanoparticles have needle shapes and sizes that are not consistent. In supporting this, XRD characterization found that incorporating GO into the nanoparticles resulted in a lower texture coefficient for ZnO (10% GO). This could be attributed to the electrochemical growth of ZnO nanocrystals onto the prominent GO sheets[32].

BET Analysis

The BET method determined the photocatalyst's surface area, average pore radius, and pore volume. In this study, the specific surface area refers to the region of active absorption on the surface of the Cu_2O/ZnO/GO nanocomposites photocatalyst when nitrogen gas is applied. The larger the active absorption area of the nanocomposite, the higher the contact between the reactants and the catalyst surface, enhancing the rate of MB degradation. Along with the nanocomposite's specific surface area, the pore size and volume can support MB molecules in entering and attaching to the surface of the Cu_2O/ZnO/GO nanocomposite catalytic pores. Table 2 shows the BET characterization.

Table 2. BET characterization of Cu_2O/ZnO/GO nanocomposites.

Sample	Specific surface area (m^2 g^{-1})	Average pore radius (Å)	Pore volume (cm^3 g^{-1})
Cu_2O/ZnO/GO 1%	26.291	15.434	0.103
Cu_2O/ZnO/GO 3%	26.780	15.434	0.100
Cu_2O/ZnO/GO 5%	35.115	19.073	0.094
Cu_2O/ZnO/GO 10%	35.874	19.073	0.092

Note: Cu_2O:ZnO = 1:2

Because of the incorporation of GO doping, the specific surface area of the Cu_2O/ZnO/GO photocatalyst increased from 26.291 m^2 g^{-1} (1% GO) to 35.874 m^2 g^{-1} (10% GO). In conjunction with the incorporation of GO doping, the same trend can be seen in the average pore size. The pore volume, on the other hand, goes from 0.103 cm^3 g^{-1} (1% GO) to 0.092 cm^3 g^{-1} (10% GO), a significant decrease. This is because of the cross-linking between the Cu_2O/ZnO and hexagonal GO groups. This cross-linking creates a relatively covalent solid bond on the pore surface in a sheet, effectively covering large pores with an active catalyst site. In addition, these results are also supported by Tantubay et al.[33], who stated that adding rGO in CuO/ZnO nanoparticles significantly improved the specific surface area. Consequently, it can be inferred that the GO composition variations in this research impacted the nanocomposite's capability to oxidize the MB compound to the most significant potential extent.

FTIR Characterization

The addition of GO dopant variations to Cu_2O/ZnO/GO nanocomposites showed no effect on the functional groups, as observed by FTIR. The GO dopant in the nanocomposite is a stabilizer for forming Cu_2O and ZnO nanoparticles and a component for filling large cavities generated during the process. Apart from functioning as a filler, GO has no impact on the chemical structure of the Cu_2O/ZnO/GO nanocomposites in any way. This is consistent with the results of the FTIR characterization of Cu_2O/ZnO/GO nanocomposites presented in Fig. 3, specifically at wavenumbers around 1390 and 1590 cm^{-1}. At wavenumber 1390 cm^{-1}, there are observed bending vibrations of the Zn-O bond [34]. In addition, the band at 1590 cm^{-1} can be attributed to the presence of the symmetric stretching of the Cu-O bond[35].

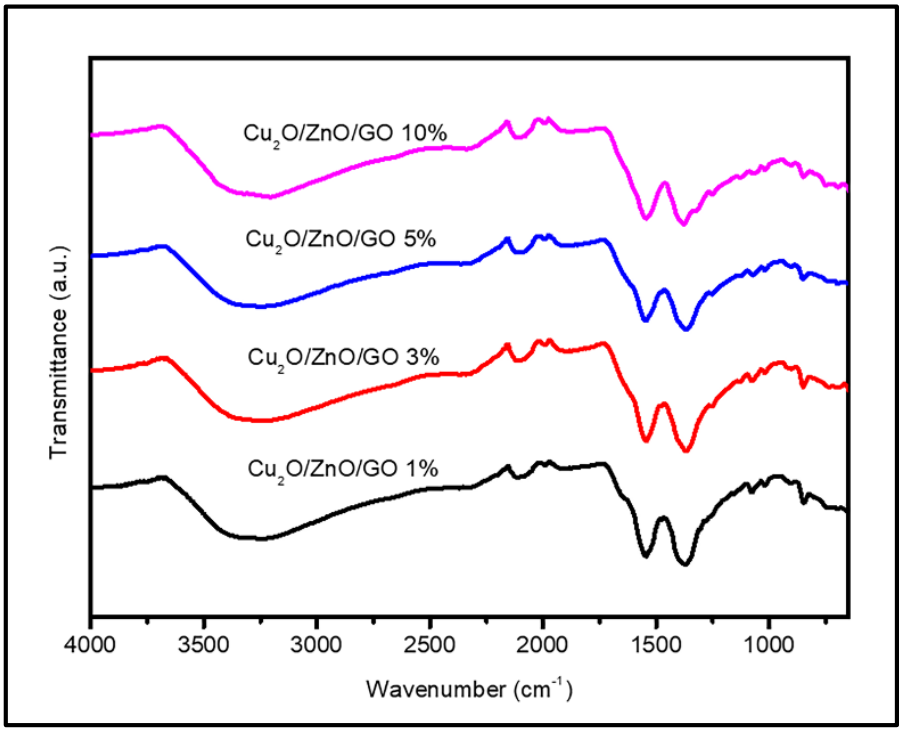

Figure 3. FTIR spectra of Cu_2O/ZnO/GO nanocomposites (Cu_2O:ZnO = 1:2) with variations of GO.

Degradation of MB

The photocatalytic degradation of MB by Cu_2O/ZnO/GO nanocomposites was monitored using a UV-Vis spectrometer, as resulted in Fig. 4. At first sight, it appeared as though the absorbance value decreased over time, but the trend was not constant. Table 3 shows the absorbance values more accurately.

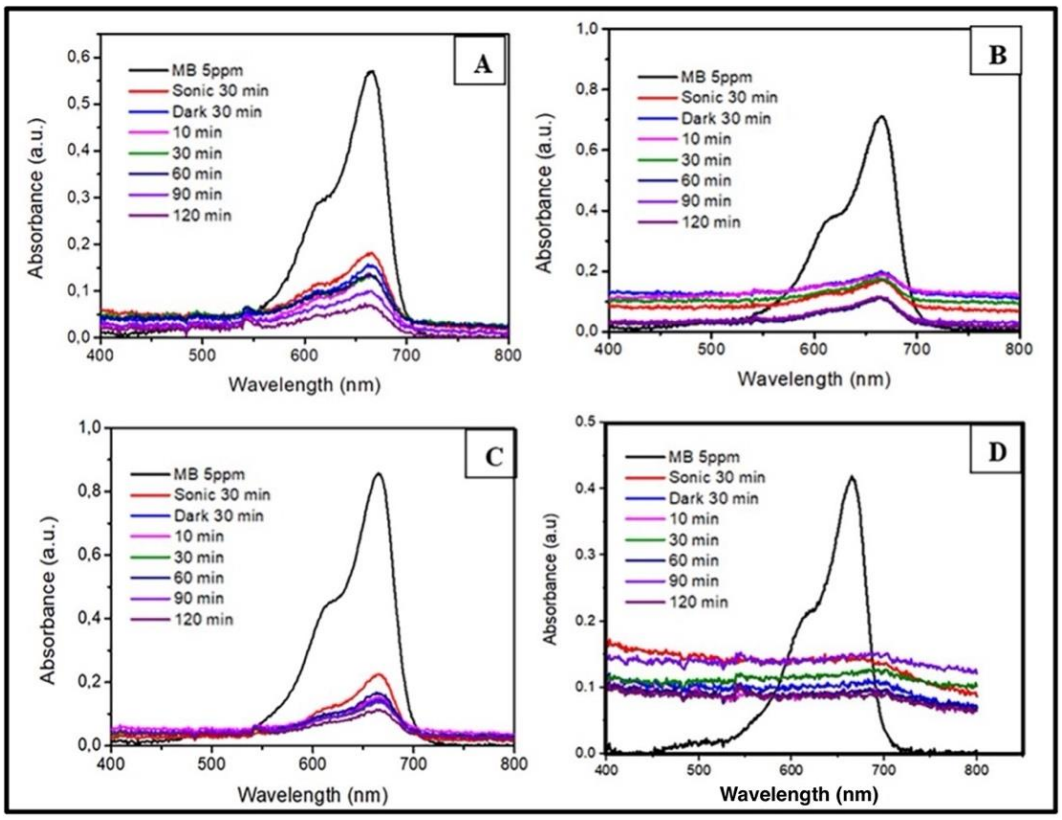

Figure 4. Absorbances during the photocatalytic degradation of MB using Cu_2O/ZnO/GO nanocomposites (Cu_2O:ZnO = 1:2) with variations of GO at (A) 1%, (B) 3%, (C) 5%, and (D) 10%.

Table 3. Absorbance values obtained during photocatalysis of MB using Cu_2O/ZnO/GO nanocomposites.

Treatment	Absorbance values			
	1% GO	3% GO	5% GO	10% GO
MB 5 ppm	0.571	0.709	0.851	0.414
Sonication	0.182	0.171	0.224	0.141
Darkness	0.154	0.194	0.143	0.108
Halogen 10 min	0.138	0.188	0.151	0.094
Halogen 30 min	0.134	0.175	0.138	0.121
Halogen 60 min	0.137	0.110	0.164	0.094
Halogen 90 min	0.099	0.114	0.137	0.149
Halogen 120 min	0.052	0.110	0.115	0.088

Note: ratio of Cu_2O:ZnO was 1:2, wavelength 664 nm, the volume of MB was 40 mL, and each increment was 4 mL.

Determining the absorbance value for the Cu_2O/ZnO/GO treatment with the 10% GO concentration proved challenging. On the surface of the Cu_2O/ZnO/GO nanocomposites, there may have been material defects that prevented the photocatalyst from functioning as it should have. When the nanocomposite was exposed to radiation from a halogen lamp, this resulted in the formation of many holes as well as electron pairs within the material. Some electron and hole pairs cannot pair successfully because they cannot move to the particle surface and interact with the MB. This prevents those electron and hole pairs from successfully pairing.

Photoluminescence Analysis

The photoluminescence test measured the photocatalyst's ability to degrade MB compounds by photocatalysis. The addition of doping material in GO has a varied influence on the degradation process for each composition variation of the nanocomposites, as illustrated in Fig. 5. The degradation percentages based on these data were 82.0%, 86.0%, 91.4%, and 79.3% for Cu_2O/ZnO/GO 1%, 3%, 5%, and 10%, respectively.

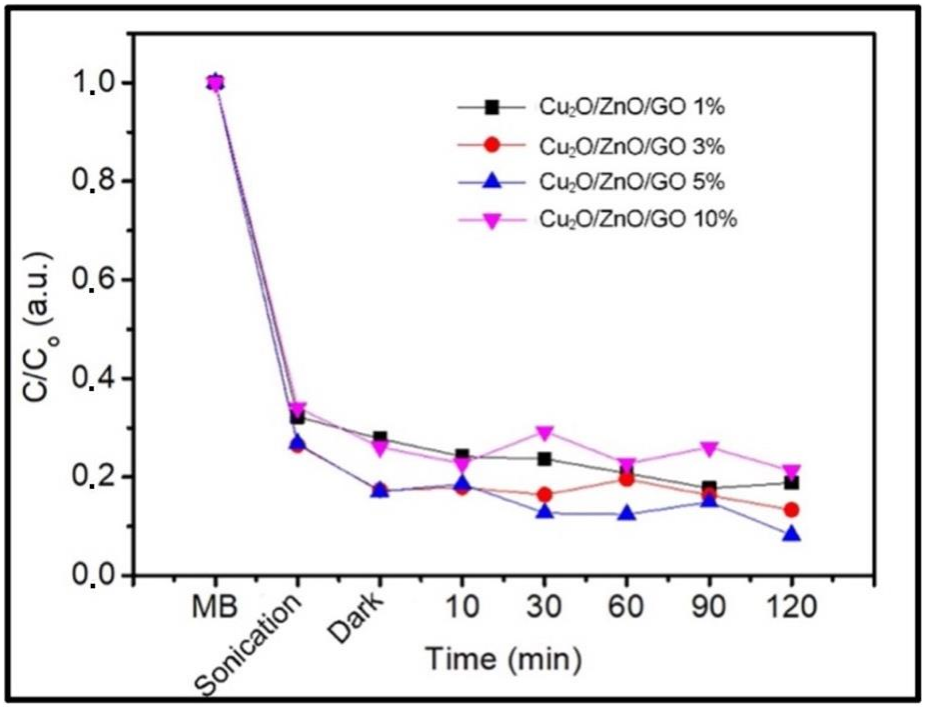

Figure 5. Photodegradation trend of MB using Cu_2O/ZnO/GO nanocomposites (Cu_2O:ZnO = 1:2) with different variations of GO.

The introduction of GO into the crystal structure causes an increase in the number of defect sites, reducing the photocatalyst material's capacity to absorb light. This is demonstrated by the results of photoluminescence testing, which are depicted in Fig. 5. These tests showed that 120 minutes of exposure to UV light resulted in the highest MB degrading efficiency of 91.4% for Cu_2O/ZnO/GO

5% nanocomposite, with the changes of C/C_o from 1 being 0.086. This is because the valence band contains an extra band that acts as the tail states. This causes the excitation of electrons to occur more slowly at lower photon energy levels, reducing the band gap's energy value (Eg). An energy band gap of 1.85 eV has been found in the synthesized nanocomposite. The photocatalytic process will be more effective if the material used as the photocatalyst has a lower band gap energy. This will allow for more significant photon and electron excitation absorption. In addition, because GO has a large active surface area on Cu_2O/ZnO/GO nanocomposites, these nanocomposites have an increased ability to conduct electricity. During the photocatalytic process, electrons in the valence band became excited, which resulted in the formation of holes. The photogenerated holes will then directly oxidize methylene blue into reactive intermediates, or they will react with hydroxyl ion (OH^-) from water, resulting in a highly oxidizing agent of hydroxyl radicals (OH·), which will complete the photocatalytic reaction. Both reactions are possible[36].

The photodegradation process initiated by the nanocomposites in this study commenced with the absorption of photons by Cu_2O and ZnO. In sequence, there is a reduction of oxygen, followed by the neutralization of OH- ions by positive holes to form OH·, neutralization of oxygen by protons, then leading to the formation of hydrogen peroxide, and finally, the decomposition of hydrogen peroxide. MB dye degradation can occur through three distinct mechanisms: oxidative decomposition of the organic matter catalyzed by hydroxyl radicals (OH·), direct oxidation by hole-electron pairs, and direct reduction through electron-ion interactions as oxidation with anionic radical superoxide species.

Conclusion:

In this study, the optimum percentage of GO dopants added in a Cu_2O/ZnO/GO nanocomposite (Cu_2O:ZnO = 1:2) for MB degradation was 10%. According to the results of BET analysis, this nanocomposite's specific surface area, pore radius, and pore volume were 35.874 $m^2\ g^{-1}$, 1.9073 nm, and 0.092 $cm^3\ g^{-1}$, respectively. Furthermore, the photocatalysis process degraded MB up to 82.0%, 86.0%, 91.4%, and 79.3% using the Cu_2O/ZnO nanocomposites (Cu_2O:ZnO = 1:2) with GO of 1%, 3%, 5%, and 10%, respectively. This study presents insights for potential future studies to examine the efficacy of this nanocomposite in the degradation of other dyes. Additionally, other researchers may also evaluate the selectivity of this material for a variety of dyes.

Acknowledgment:

The authors would like to thank the Nanomaterials for Renewable Energy (NRE) Laboratorium (CV. Inovasi Teknologi Nano) for the support, guidance, and facilities during this research.

Authors' Declaration:

- Conflicts of Interest: None.
- We hereby confirm that all the Figures and Tables in the manuscript are ours. Besides, the Figures and Images, which are not ours, have been given the permission for re-publication attached with the manuscript.
- The authors signed an animal welfare statement.
- Ethical Clearance: The project was approved by the local ethical committee in Universitas Sumatera Utara.

Authors' Contribution Statement:

F. J. P. developed the study design and conducted the experiment. K. T. applied the concepts and methodologies. Z. S. analyzed and interpreted the data. N. S. wrote the manuscript and made revisions.

References:

1. Haseeb M, Haouas I, Nasih M, et al. Asymmetric impact of textile and clothing manufacturing on carbon-dioxide emissions: Evidence from top Asian economies. Energy. 2020; 196: 117094. https://doi.org/10.1016/j.energy.2020.117094
2. Ismail M, Akhtar K, Khan MI, Kamal Tahseen , Khan A Murad Asiri M Abdullah, et al. Pollution, Toxicity and Carcinogenicity of Organic Dyes and their Catalytic Bio-Remediation. Curr Pharm. 2019; 25: 3645–3663. https://doi.org/10.2174/1381612825666191021142026
3. Shindhal T, Rakholiya P, Varjani S, Pandey Ashok, Guo Wenshan Hao Ngo Huu, et al. A critical review on advances in the practices and perspectives for the treatment of dye industry wastewater. Bioengineered. 2021; 12: 70–87. https://doi.org/10.1080/21655979.2020.1863034
4. Nandhini NT, Rajeshkumar S, Mythili S. The possible mechanism of eco-friendly synthesized nanoparticles on hazardous dyes degradation. Biocatal Agric Biotechnol. 2019; 19: 101138. https://doi.org/10.1016/j.bcab.2019.101138
5. Salgot M, Folch M. Wastewater treatment and water reuse. Curr Opin Environ Sci Health. 2018; 2: 64–74. https://doi.org/10.1016/j.coesh.2018.03.005
6. Ali SS, Sun J, Koutra E, El-Zawawy Nessma , Elsamahy Tamer El-Shetehy Mohamed.

Construction of a novel cold-adapted oleaginous yeast consortium valued for textile azo dye wastewater processing and biorefinery. Fuel. 2021; 285: 119050. https://doi.org/10.1016/j.fuel.2020.119050

7. Sarayu K, Sandhya S. Current Technologies for Biological Treatment of Textile Wastewater–A Review. Appl Biochem Biotechnol. 2012; 167: 645–661. https://doi.org/10.1007/s12010-012-9716-6
8. Miklos DB, Remy C, Jekel M, Linden Karl G, Drewes Jörg E, Hübner Uwe, et al. Evaluation of advanced oxidation processes for water and wastewater treatment – A critical review. Water Res. 2018; 139: 118–131. https://doi.org/10.1016/j.watres.2018.03.042
9. Laghrib F, Bakasse M, Lahrich S, El Mhammedi Moulay Abderrahim . Advanced oxidation processes: photo-electro-Fenton remediation process for wastewater contaminated by organic azo dyes. Int J Environ Anal Chem. 2021; 101: 2947–2962. https://doi.org/10.1080/03067319.2020.1711892
10. Singla S, Sharma S, Basu S, Shetti P Nagaraj, Aminabhavi Tejraj M. Photocatalytic water splitting hydrogen production via environmental benign carbon based nanomaterials. Int J Hydrogen Energy. 2021; 46: 33696–33717. https://doi.org/10.1016/j.ijhydene.2021.07.187
11. Li P, Li D, Liu L, Li Anli, Luo Cuixian, Xiao Yue, et al. Concave structure of Cu_2O truncated microcubes: PVP assisted {100} facet etching and improved facet-dependent photocatalytic properties. CrystEngComm. 2018; 20: 6580–6588. https://doi.org/10.1039/C8CE01332B
12. Kerour A, Boudjadar S, Bourzami R, Allouche B. Eco-friendly synthesis of cuprous oxide (Cu_2O) nanoparticles and improvement of their solar photocatalytic activities. J Solid State Chem. 2018; 263: 79–83. https://doi.org/10.1016/j.jssc.2018.04.010
13. Singh J, Juneja S, Soni RK, Bhattacharya Jaydeep . Sunlight mediated enhanced photocatalytic activity of TiO_2 nanoparticles functionalized CuO-Cu2O nanorods for removal of methylene blue and oxytetracycline hydrochloride. J Colloid Interface Sci. 2021; 590: 60–71. https://doi.org/10.1016/j.jcis.2021.01.022
14. Nie J, Li C, Jin Z, Hu Wen-ting, Wang Jia-hao, , Huang Ting, et al. Fabrication of MCC/Cu_2O/GO composite foam with high photocatalytic degradation ability toward methylene blue. Carbohydr Polym. 2019; 223: 115101. https://doi.org/10.1016/j.carbpol.2019.115101
15. Huo Y, Wang Z, Zhang J, Liang Changhao Dai Kai . Ag SPR-promoted 2D porous g-C_3N_4/Ag_2MoO_4 composites for enhanced photocatalytic performance towards methylene blue degradation. Appl Surf Sci. 2018; 459: 271–280. https://doi.org/10.1016/j.apsusc.2018.08.005
16. Wang P, Qi C, Hao L, Wen Pengchao , Xu Xin . Sepiolite/Cu_2O/Cu photocatalyst: Preparation and high performance for degradation of organic dye. J Mater Sci Technol. 2019; 35: 285–291. https://doi.org/10.1016/j.jmst.2018.03.023
17. Zhang D, Yang J, Wang J, Yang Jianfeng, Qiao Guanjun . Construction of Cu_2O-reduced graphene oxide composites with enhanced photoelectric and photocatalytic properties. Opt Mater (Amst). 2020; 100: 109612. https://doi.org/10.1016/j.optmat.2019.109612
18. Muscetta M, Jitan S al, Palmisano G, Andreozzi Roberto, Marotta Raffaele, Cimino Stefano et al. Visible light – driven photocatalytic hydrogen production using Cu_2O/TiO_2 composites prepared by facile mechanochemical synthesis. J Environ Chem Eng. 2022; 10: 107735. https://doi.org/10.1016/j.jece.2022.107735
19. Gao S, Zhang H, Wang X, Deng Ruiping, Sun Dehui, Zheng Guoli. ZnO-Based Hollow Microspheres: Biopolymer-Assisted Assemblies from ZnO Nanorods. J Phys Chem B. 2006; 110: 15847–15852. https://doi.org/10.1021/jp062850s
20. Fatima R, Kim J-O. Inhibiting photocatalytic electron-hole recombination by coupling MIL-125(Ti) with chemically reduced, nitrogen-containing graphene oxide. Appl Surf Sci. 2021; 541: 148503. https://doi.org/10.1016/j.apsusc.2020.148503
21. Zhang Y-H, Cai X-L, Guo D-Y, Zhang Hui-Jing Zhou Ning, Fang Shao-Ming, et al. Oxygen vacancies in concave cubes Cu_2O-reduced graphene oxide heterojunction with enhanced photocatalytic H2 production. J Mater Sci: Mater Electron. 2019; 30: 7182–7193. https://doi.org/10.1007/s10854-019-01036-2
22. Zou W, Zhang L, Liu L, Wang Xiaobo, Sun Jingfang, Wu Shiguo et al. Engineering the Cu_2O–reduced graphene oxide interface to enhance photocatalytic degradation of organic pollutants under visible light. Appl Catal B. 2016; 181: 495–503. https://doi.org/10.1016/j.apcatb.2015.08.017
23. Ma J, Wang K, Li L, Zhang Tianli, Kong Yong, Komarneni Sridhar, et al. Visible-light photocatalytic decolorization of Orange II on Cu_2O/ZnO nanocomposites. Ceram Int. 2015; 41: 2050–2056. https://doi.org/10.1016/j.ceramint.2014.09.137
24. Huang H, Zhang J, Jiang L, Zang Zhigang . Preparation of cubic Cu_2O nanoparticles wrapped by reduced graphene oxide for the efficient removal of rhodamine B. J Alloys Compd 2017; 718: 112–115. https://doi.org/10.1016/j.jallcom.2017.05.132
25. Purba FJ, Tarigan K, Sitorus Z, Nurdin Iregar, Ema Frida, Nurdin Bukit, et al. Cu_2O/ZnO Nanocomposite and Graphene Oxide with Photocatalysis for Textile Dyes/Dye Reduction. Tianjin Daxue Xuebao. 2022; 55: 388–398. https://doi.org/10.17605/OSF.IO/3JD56
26. Regmi A, Bhandari J, Bhattarai S, Gautam K Surendra. Synthesis, Characterizations and Antimicrobial Activity of Cuprous Oxide (Cu_2O) Nanoparticles. J Nepal Chem Soc. 2019; 40: 5–10. https://doi.org/10.3126/jncs.v40i0.27271

27. Hjiri M, Mir L, Leonardi S. Synthesis, Characterization and Sensing Properties of AZO and IZO Nanomaterials. Chemosensors. 2014; 2: 121–130. https://doi.org/10.3390/chemosensors2020121
28. Yoo MJ, Park HB. Effect of hydrogen peroxide on properties of graphene oxide in Hummers method. Carbon. 2019; 141: 515–522. https://doi.org/10.1016/j.carbon.2018.10.009
29. Scherrer P. Bestimmung der Grösse und der inneren Struktur von Kolloidteilchen mittels Röntgenstrahlen. Nachrichten von der Gesellschaft der Wissenschaften zu Göttingen, mathematisch-physikalische Klasse 1918; 98–100.
30. Zhang W, Xu H, Xie F, Ma Xiaohua, Niu Bo, Mingqi Chen et al. General synthesis of ultrafine metal oxide/reduced graphene oxide nanocomposites for ultrahigh-flux nanofiltration membrane. Nat Commun. 2022; 13: 471. https://doi.org/10.1038/s41467-022-28180-4
31. Islam MR, Rahman M, Farhad SFU, Podder J. Structural, optical and photocatalysis properties of sol–gel deposited Al-doped ZnO thin films. Surf Interfaces. 2019; 16: 120–126. https://doi.org/10.1016/j.surfin.2019.05.007
32. Rosas-Laverde NM, Pruna A, Busquets-Mataix D, Marí B, Cembrero J, Vicente F Salas, et al. Improving the properties of Cu_2O/ZnO heterojunction for photovoltaic application by graphene oxide. Ceram Int. 2018; 44: 23045–23051. https://doi.org/10.1016/j.ceramint.2018.09.107
33. Tantubay K, Das P, Baskey Sen M. Ternary reduced graphene oxide–CuO/ZnO nanocomposite as a recyclable catalyst with enhanced reducing capability. J Environ Chem Eng. 2020; 8: 103818. https://doi.org/10.1016/j.jece.2020.103818
34. Phoohinkong W, Foophow T, Pecharapa W. Synthesis and characterization of copper zinc oxide nanoparticles obtained via metathesis process. Advances in Natural Sciences: Nanoscience and Nanotechnology. 2017; 8: 035003. https://doi.org/10.1088/2043-6254/aa7223
35. Al-Senani GM, Al-Saeedi SI, Al-Kadhi NS, Abd-Elkader Omar H Deraz Nasrallah M. Green Synthesis and Pinning Behavior of Fe-Doped CuO/Cu_2O/Cu_4O_3 Nanocomposites. Processes. 2022; 10: 729. https://doi.org/10.3390/pr10040729
36. Ma Z, Hu L, Li X, Deng Lingjuan, Fan Guang He Yangqing. A novel nano-sized MoS_2 decorated Bi_2O_3 heterojunction with enhanced photocatalytic performance for methylene blue and tetracycline degradation. Ceram Int. 2019; 45: 15824–15833. https://doi.org/10.1016/j.ceramint.2019.05.085

النشاط التحفيزي المعزز للمركبات النانوية Cu_2O / ZnO / GO على تحلل الميثيلين الأزرق

فريكسون جوني بوربا [1] زوريا سيتوروس [1] يريستا تاريجان [1] نور الدين سيرغار [2]

[1]قسم الفيزياء ، كلية الرياضيات والعلوم الطبيعية ، جامعة سومطرة أوتارا ، بادانج بولان ، 20155 ، ميدان ، إندونيسيا.
[2]قسم الفيزياء ، كلية الرياضيات والعلوم الطبيعية ، جامعة نيجري ميدان ، كينانجان بارو ، 20221 ، ميدان ، إندونيسيا.

الخلاصة:

في هذا البحث، مادة التحفيز الضوئي للمركبات النانوية مركبة من مخلوط الجسميات النانوية Cu_2O، والجسميات النانوية ZnO و أكسيد الغرافين (GO) من خلال منهجي الترسيب المتشارك والهيدروحراري. يهدف هذا البحث إلى معرفة التكوينات المثلى من المركبات النانوية Cu_2O/ZnO/GO لانحلال الميثيلين الأزرق. ويقام تركيب المركبات النانوية بخطوتين: (1) تركيب المركبات النانوية Cu_2O و ZnO بمنهج الترسيب المتشارك وتحضير GO من خلال منهاج هامر المعدل؛ (2) تحضير مخلوط الجسميات النانوية لمركبات النانوية مع GO من خلال المنهج الهيدروحراري لشكل المركبات النانوية Cu_2O/ZnO/GO. ويقام عملية امتزاز التحفيز الضوئي على الميثيلين الأزرق بمساعدة الأشعة فوق البنفسجية من مصباح الهالوجين. تدل نتائج الخصائص على أن التكوينات المثلى هي المركبات النانوية Cu_2O/ZnO مع نسبة 1:2.و10% من GO وله مساحة محددة 35.874 $م^2$ $ج^{-1}$، ونصف قطر مسامي 19.073 نانومتر، وحجم المسام 0.092 $سم^3$ $ج^{-1}$، وحجم البلورة 31.19 نانومتر. كانت كفاءة تحلل الميثيلين الأزرق تحت ضوء الأشعة فوق البنفسجية لمدة 120 دقيقة 82.0٪ ، 86.0٪ ، 91.4٪ ، و 79.3٪ باستخدام المركبات النانوية Cu_2O/ZnO مع GO بنسبة 1٪ ، 3٪ ، 5٪ ، و 10٪ على التوالي .وأيضا، هذه النتائج تدل على أن المركبات النانوية Cu_2O/ZnO/GO تعطي الكفاية المرضية في انحلال الميثيلين الأزرق من نفايات صبغ النسيج.

الكلمات المفتاحية: أكسيد الجرافين، الميثيلين الأزرق، المركبات النانوية، عملية التحفيز الضوئي، انحلال نفايات صبغ النسيج.